Hindawi Publishing Corporation
Advances in Materials Science and Engineering
Volume 2015, Article ID 678739, 7 pages
http://dx.doi.org/10.1155/2015/678739

Research Article

Preparation and Characterization of Nickel Ferrite-SiO_2/Ag Core/Shell Nanocomposites

I. G. Blanco-Esqueda,[1] G. Ortega-Zarzosa,[1] J. R. Martínez,[1,2] and A. L. Guerrero[3]

[1]*Facultad de Ciencias, Universidad Autónoma de San Luis Potosí, Álvaro Obregón No. 64, Colonia Centro, 78000 San Luis Potosí, SLP, Mexico*
[2]*Departamento de Físico-Matemáticas, Universidad Autónoma de San Luis Potosí, Álvaro Obregón No. 64, Colonia Centro, 78000 San Luis Potosí, SLP, Mexico*
[3]*Instituto de Física, Universidad Autónoma de San Luis Potosí, Álvaro Obregón No. 64, Colonia Centro, 78000 San Luis Potosí, SLP, Mexico*

Correspondence should be addressed to A. L. Guerrero; azdlobo@gmail.com

Received 2 July 2015; Revised 10 October 2015; Accepted 15 October 2015

Academic Editor: Antonio Riveiro

Magnetic composites with silver nanoparticles bonded to their surface were successfully prepared using a simple chemical method. By means of a sol-gel technique, nickel ferrite nanoparticles have been prepared and coated with silica to control and avoid their magnetic agglomeration. The structural and magnetic properties of the nanoparticles were studied in function of the annealing temperature. Then, silver nanoparticles were incorporated by hydrolysis-condensation of tetraethyl orthosilicate, which contains silver nitrate on the surface of the nickel ferrite-SiO_2 core/shell. Samples were characterized using X-ray diffraction, IR spectroscopy, SEM, and magnetometry. Results show that the silica covered the nickel ferrite nanoparticles and the silver nanoparticles remain stable in the surface of the composite.

1. Introduction

Nickel ferrite is an important magnetic material with a variety of applications, such as fabrication of ferrofluids, catalysis, and magnetic refrigeration [1, 2], and is one of the most important soft ferrites with high electromagnetic performance, low coercivity, good mechanical hardness, and chemical stability [3].

The nickel ferrite is obtained by sol-gel process followed by thermal treatment above 1000°C, which is the temperature of crystallization reported in previous works [4, 5]. The crystal structure of the obtained ferrites is neither a simple NaCl-type nor a simple spinel type. The average structure can be described in the space group Fd3m, but additional octahedral sites, with respect to the spinel structure, are partially occupied whenever an excess of divalent cation is used [6]. Instead of getting materials of formula $NiFe_2O_4$, some irons may be missing and some extra divalent cations have been incorporated, the final formula can be expressed as $Ni_{1+x}Fe_{2-2x/3}O_4$, with x being 0.43 [6, 7].

The nickel ferrite presents similar magnetic properties to magnetite and maghemite [4]. However, these nanoparticles tend to agglomerate and oxidize. In order to avoid this, a coat of silica or some polymers is used to cover the nanoparticles [5, 8–10]. In this sense, sol-gel is a simple method that produces stable nanoparticles embedded in a silica matrix, simultaneously providing the synthesis of nickel ferrite and their silica cover, so that any coating technique on magnetic nanoparticles is unnecessary.

On the other hand, the silver nanoparticles have attracted considerable attention because of their catalytic, optical, and transport properties and bactericidal activity against *Escherichia coli*, *Staphylococcus epidermis*, and *Bacillus subtilis* [11, 12].

Given the bactericidal property of Ag nanoparticles, magnetic composites functionalized with these nanoparticles in

their surface could be efficiently used for cleaning and purification of aqueous medium and environmental remediation. Also, these composites can be easily recovered using a magnetic field avoiding the negative effect of the nanoparticles on ecosystems. In addition to these two characteristics, they might exhibit strong microwave adsorption and SERS phenomena and could be candidates for cancer therapy and so on [13–19].

The use of a magnetic carrier has become a promising choice for the isolation and removal of environmental contaminants or undesirable substances in water or other media, with the advantage that the magnetic composite used to disinfect can be recovered using an external magnetic field, which inhibit its impact on the environment. In this work we present a simple chemical method to incorporate silver nanoparticles to a composite formed by the nickel ferrite covered with SiO_2 and obtain an antibacterial agent fixed to a magnetic carrier.

2. Experimental

2.1. Nickel Ferrite-SiO_2 Preparation. The samples were prepared by sol-gel method using tetraethyl orthosilicate, $Si(OC_2H_5)_4$ (TEOS), as a precursor of the silica [20]; distilled water and ethanol (Et-OH) were also used in the preparation stage. Considering that the silica structure strongly depends on the H_2O/TEOS ratio and according to previous results a proportion of H_2O = 1/TEOS = 11.6/Et-OH = 4 was used to ensure a full hydrolyzation [21]. On the other hand, nickel chloride ($NiCl_2{\cdot}6H_2O$) and iron chloride ($FeCl_3{\cdot}6H_2O$) were used in order to form the nickel ferrite phase. To prepare the nickel ferrite-SiO_2 composite, first 10.2 mL of TEOS was mixed with 10.45 mL of ethanol and the solution was stirred for 10 minutes and then another solution containing 1.1715 g of $NiCl_2{\cdot}6H_2O$, 1.332 g, $FeCl_3{\cdot}6H_2O$, and 8.0 mL of distilled water is prepared to finally mix this second solution with the first one and stirred during 5 minutes. Thereafter the sample was left to gelation at room temperature for several hours.

The obtained gel was annealed for 1 h at 400, 800, and 1100°C of air temperature. Samples were identified as follows: without heat treatment (A) and annealing at 400°C (B), at 800°C (C), and at 1100°C (D). A direct relationship between obscuration and temperature increase is observed which happens to be an indicator of the crystallization of the nickel ferrite. In Figure S1 of the Electronic Supplementary Information (S1-ESI) (see Supplementary Material available online at http://dx.doi.org/10.1155/2015/678739) a micrograph of the nickel ferrite, with a small cover of silica and before the functionalization with Ag, is shown.

2.2. Nickel Ferrite-SiO_2/Ag Preparation. Once the nickel ferrite nanoparticles were formed with their coat of SiO_2, the Ag nanoparticles were adhered to the composite surface by a simple chemical method which involves reduction of the Ag nanoparticles and binding them on the SiO_2 surface. This process begins by mixing and stirring 4 mL of tetramethylammonium hydroxide (TMAOH) and 0.8 mL of tetraethyl orthosilicate (TEOS) with 0.1 g of the composites formed by the nickel ferrite and the silica during 10 min. Then, 6.0 mL of silver nitrate at 0.01 M is added and stirring continues for over 30 minutes. Finally, to reduce the Ag nanoparticles, 6.0 mL of sodium borohydride ($NaBH_4$) at 0.2 M was added and stirred for 30 min. Thereby when the $NaBH_4$ is added, an effervescent reaction between the silver nanoparticles and the surface of the composites occurs and the Ag nanoparticles grow on the SiO_2 surface of the composites. Finally, composites were washed several times with deionized water and dried at room temperature.

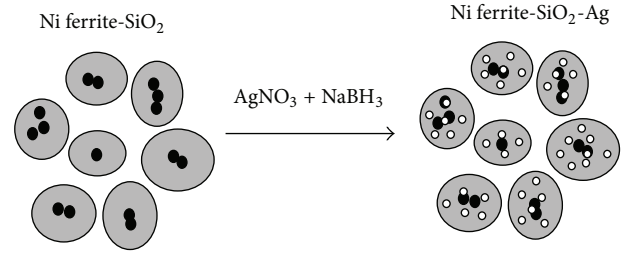

Figure 1: Incorporation of silver particles to silica coated nickel ferrite.

Although the mechanisms allowing silver to adhere to the surface of SiO_2 are not completely understood yet, the evidence indicates that these nanoparticles are not covered by the silica and therefore the antibacterial activity of the Ag remains present on the nanoparticles as shown in (Figure S2, ESI).

Thus we can obtain nickel ferrite-SiO_2 composites, where clusters of nickel ferrite nanoparticles are in the core with a cover of SiO_2, and the Ag nanoparticles would then incorporate on the surface of the composite, as is schematized in Figure 1.

2.3. Characterization. The structural properties and the incorporation of Ag on the composite were studied using X-ray diffraction, the patterns were obtained using a GBC-Difftech MMA diffractometer with filtered CuKα (λ = 1.54 Å) radiation. The refinement was fitted using the MAUD program [22]. In the initial model of the refinement, the nonstoichiometric nickel ferrite ($Ni_{1.43}Fe_{1.7}O_4$) with cubic symmetry and spatial group Fd-3m:1 is used in agreement with the information provided in [6]. In addition, the trigonal structure and spatial group $P3_12_1$ are assumed for the amorphous phase of silica (SiO_2). The silica coating was analyzed by IR spectra which also corroborated the Ag incorporation. IR spectra were obtained using Nicolet Avatar 360 as equipment, and a potassium bromide pastille with approximate 5% volume of sample was prepared. The behavior of the nickel ferrite was studied by magnetometry using an alternating gradient magnetometer Micromag, AGM 2900 of Princeton Measurements, through which the hysteresis loops were obtained. SEM examinations and EDS analysis were carried out by using an XL-30 SEM (Philips, Netherlands) and a DX-41 (EDAX), respectively.

3. Results and Discussion

In the coated samples with silica, the X-ray patterns, Figure 2(a), show a broad peak around 23° which shifts left

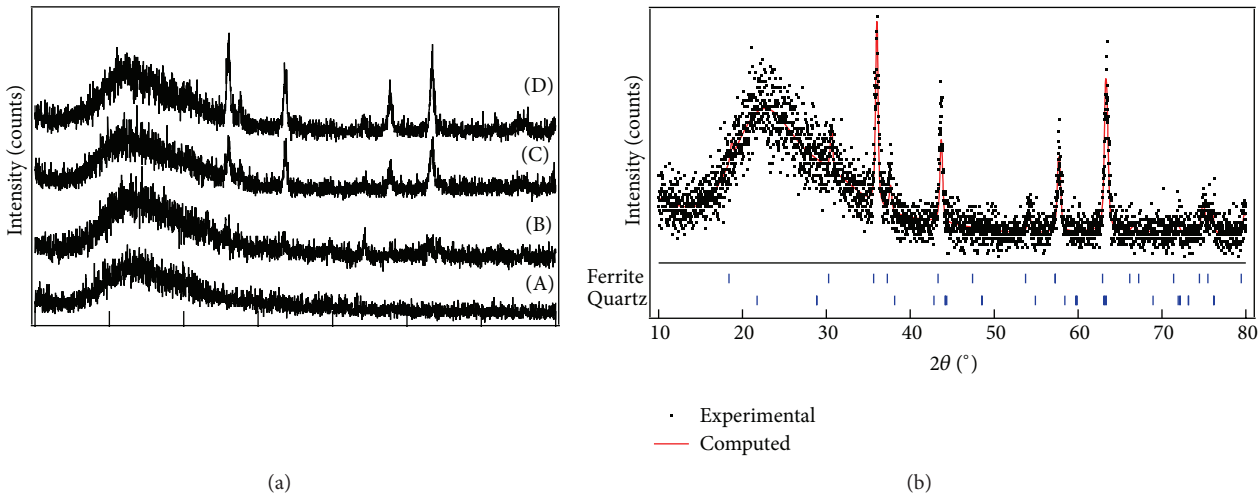

FIGURE 2: X-ray diffractograms of silica coated nickel ferrite at (a) various calcination temperatures and (b) Rietveld refinement of sample D.

when temperature increases; this broad peak corresponds to the SiO_2 amorphous phase [4, 23]. This behavior is an indication that the amorphous structure is rearranged due to annealing temperature [24, 25].

In sample (A) there is no evidence of any crystalline structure; only the amorphous behaviour of the silica is identified. For sample (B) incipient peaks were identified at 36.5°, 44°, 57°, and 63.5°; these peaks match with the nickel ferrite, $Ni_{1.43}Fe_{1.7}O_4$, but their intensity is low. When the temperature of the heat treatment increases above 800°C, samples (C) and (D), we can see well-defined peaks at positions which correspond to these iron oxides, in particular those peaks corresponding to the nonstoichiometric nickel ferrite ($Ni_{1.43}Fe_{1.7}O_4$) [6, 7]. The peaks associated with the nickel ferrite are more intense, sharp, and well defined when sintering temperature is about 1100°C, indicating an increment of the nickel ferrite crystallinity, and due to the growing of the clusters conformed by the nickel ferrite nanoparticles.

Rietveld refinement analysis has been shown to also work well while calculating the amorphous/crystalline fraction in composites with crystalline phases, as in the current case [23]. In any case, very good agreement between experimental and calculated amorphous/crystalline fraction of composites was obtained [26].

Figure 2(b) shows the Rietveld refinement wherein the amorphous phase has a trigonal structure and the good adjustment indicates the presence of a silica covering. The presence of these two phases is confirmed by the Rietveld refinement for amorphous SiO_2. Using the above refinement process, the Bragg pattern and the position of the peaks in the diffractograms correspond to the phases identified according to the spatial group Fd3m:1, with cubic symmetry for the nickel ferrite $Ni_{1.43}Fe_{1.7}O_4$, and $P3_12_1$, with trigonal symmetry for the quartz-like amorphous SiO_2.

The crystal structure was refined using the Rietveld method being very well fitted with a lattice parameter of the nickel ferrite of 8.3490 ± 0.0006 Å and a crystallite size of 47.5 nm. The weight percentage of phases calculated by Rietveld refinement were 94.35 ± 2.3% of SiO_2 and 5.63 ± 0.33% of nickel ferrite. The R factors for the final refinement were R_{wp} = 4.62%, R_p = 3.54%, and R_{wpnb} = 20.4%, although the quality of the Rietveld fit can be best determined by considering both the observed and calculated graphically, which ensure that the model is chemically plausible [27]. In addition, the results obtained from the refinement of the nickel ferrite are in good agreement with the results obtained previously for this structure [6].

IR analysis was made to study the absorption bands of the nickel ferrite-SiO_2 core-shell at various heat-treated temperatures. Therefore the IR spectra shown in Figure 3 describe the bands located around 450, 800, and 1070 cm^{-1} each that are associated with the vibrations in the Si-O of rocking, bending, and stretching bonds, respectively [28]. Sample (D) shows extended well-defined bands in the range from 450 to 770 cm^{-1}; these bands have been assigned to vibrational modes of Fe-O bonds in Fe_2O_3 [4, 29]. These IR features indicate the formation of the iron oxide species at this annealing temperature. In the spectra we observed that the peaks at about 480 cm^{-1} are very sharp; this fact and the presence of the peaks at about 426, 560, 622, 776, and 837 cm^{-1}, Figure 3(b), indicate the formation of spinel phase, according to X-ray results and previous results of Ni ferrite embedded in silica xerogel matrix [30], among the features observed about 690 and 730 cm^{-1} due to structural effects over the SiO_2 caused by the presence of nickel ferrite.

With respect to the band observed around 1070 cm^{-1}, sample (A) has a shoulder around 1200 cm^{-1} which, when temperature increases, incorporates to the main band; at the same time, the band located at 950 cm^{-1}, assigned to the stretching vibrations of silanols groups [Si-(OH)] [31], incorporates to the band located at 1070 cm^{-1} when temperature increases. This forms a broad band around 1070 cm^{-1} which is attributed to the formation of colloidal oxide particles in the SiO_2 matrix [32]; their introduction produces structural disorder, reflected in the broadening of the IR band in the stretching region [21] and the appearance of rings in the

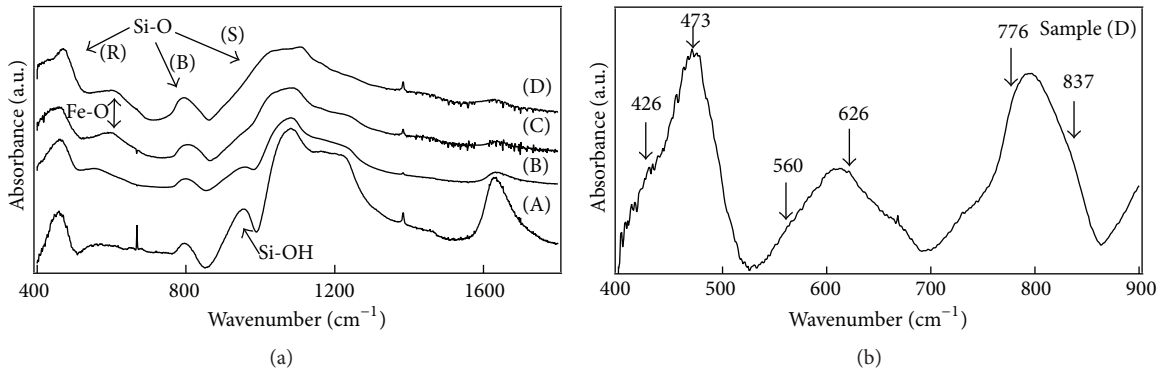

FIGURE 3: IR spectra of nickel ferrite-SiO_2 at (a) different heat treatment temperatures and (b) IR spectra in the range from 400 to 900 cm^{-1} for sample D.

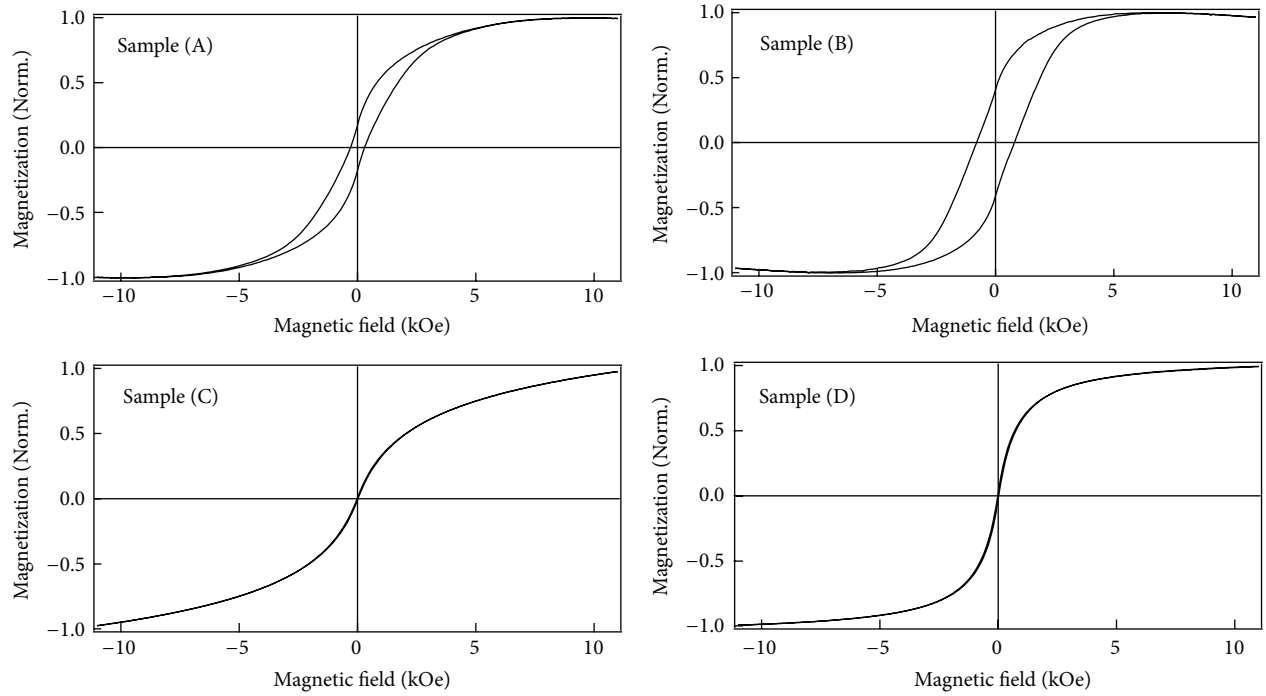

FIGURE 4: Hysteresis loop obtained for the samples: (A) without heat treatment, (B) calcined at 400°C, (C) calcined at 800°C, and (D) calcined at 1100°C.

structure of the silica xerogel [28]. On the other hand, the asymmetric band situated at 1630 cm^{-1} at spectra A has two components assigned to the deformation of the molecular water, which are probably trapped inside the voids [33, 34], and contribution about 1650 cm^{-1} that can be assigned to residual ethanol. The presence of this band indicates a high presence of hydroxyls; the band intensity decreases under heat treatment. We can observe that this band has a strong presence on samples at low annealing temperatures.

There is another band situated in 560 cm^{-1} which appears from sample (B); this band corresponds to vibrations of Fe-O and tends to shift up to 606 cm^{-1} for sample (D) that is attributed to an increment of the nickel ferrite crystallinity when sintering temperature increases [3].

Figure 4 shows the hysteresis loops of the nickel ferrite particles coated with silica. The magnetic saturation was normalized at maximum applied field (12 kOe). Samples without heat treatment (A) and calcined at 400°C (B) both show ferromagnetic behaviour, while sample (C), heat-treated at 800°C, does not reach the saturation, due to a structural inhomogeneity since nickel ferrite is not well formed yet. In the case of sample (D), saturation is reached at 5 kOe. Also, a superparamagnetic behaviour is observed in these two samples, which is attributed to the formation of the nickel ferrite phase.

These results are in agreement with the structural analysis made by X-ray diffraction and IR spectroscopy and confirm the formation of the nickel ferrite phase with high crystallinity at 1100°C. On the other hand, samples with annealing

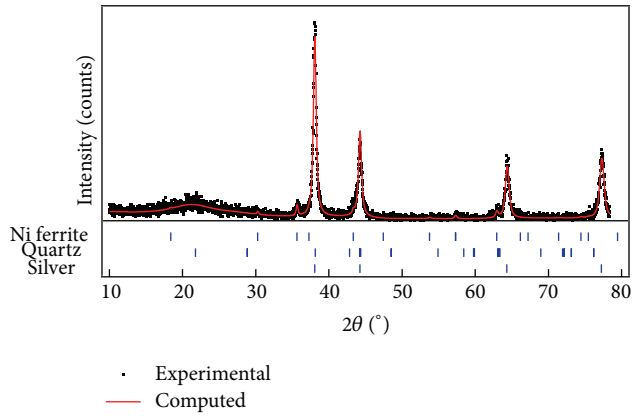

Figure 5: X-ray diffractogram and Rietveld refinement of $Ni_{1.43}Fe_{1.7}O_4$-SiO_2/Ag.

temperature below 400°C present a ferromagnetic behaviour, which is attributed to the presence of γ-Fe_2O_3 and some nickel phases before forming the nickel ferrite.

According to structural and magnetic results, sample (D) has the best magnetic properties in addition to high crystallinity degree. Therefore this sample was selected to incorporate the Ag nanoparticles, according to the experimental procedure shown in Section 2.2.

The X-ray diffractogram (Figure 5) shows the incorporation of silver to the composite formed with the nickel ferrite and SiO_2; the peaks corresponding to the nickel ferrite were overshadowed by the intensity of the peaks corresponding to elemental silver, represented by the peaks located at 38°, 44°, 65°, and 78°. In this diffractogram the peaks of nickel ferrite are obscured by the presence of the silver nanoparticles which grow in the surface of the composite [35, 36]; however, the presence of the nickel ferrite in this stage is better corroborated by the superparamagnetic properties shown in Figure 4. This superparamagnetism also indicates that nickel ferrite particles are in nanoscale size. In the refinement, we can observe the nickel ferrite peaks wherein intensity is low, due to the presence of silica as the cover shell; however, because nickel ferrite remains in the core of the composites, these nanoparticles remain untouched during the growth of silver in the SiO_2 surface of the composites.

The structural parameters for Ag are calculated by Rietveld refinement, in which the spatial group Fm-3m was used, leading to a lattice parameter of 4.0926 ± 0.0006 Å and a crystallite size of 27.4 nm, whereas for the nickel ferrite phase we obtained a particle size of 47.5 nm, with lattice parameters of 8.3490 ± 0.0006 Å, similar to the values obtained for nickel ferrite in SiO_2, which indicates the stability of the composite. For the final composites, the weight percentage of phases calculated by Rietveld refinement was $78.04 \pm 4.67\%$ of SiO_2, $3.46 \pm 0.21\%$ of nickel ferrite, and $18.49 \pm 1.11\%$ of Ag.

According to the preparation procedure, the Ag nanoparticles are located over the silica coat formed to cover the nickel ferrite nanoparticles. This configuration serves a dual purpose. On one hand, the antimicrobial agent on the surface interacts with the environment, while it is linked to the magnetic particles. On the other hand, through application of magnetic field it is possible to recover the particles. In this sense, there are some groups working on functionalizing superparamagnetic nanoparticles such as magnetite and cobalt with antibacterial agents [11, 36, 37]. However preparation and functionalization of nickel ferrite nanoparticles represent an easier process.

Figure 6 shows an SEM image in a large range where the formation of nickel ferrite-SiO_2-Ag is observed. The bright grains correspond to Ag particles over the nickel ferrite-SiO_2. Dark zone corresponds to nickel ferrite-SiO_2, with a lower presence of Ag. From the EDS results, the quantity of elements calculated for the former case indicates that the content is mainly Si, followed by O and then, in similar proportion, Ag and Fe and finally Ni, as we can observe at Figure 6(c).

In Figure 6(b), we show an isolated aggregate in which the structure of the nickel ferrite-SiO_2/Ag can be observed.

Thus, using an easy chemical route, as it is in the sol-gel technique, we can obtain the formation of nickel ferrite nanoparticles embedded in xerogel matrix. These aggregates have a core-shell structure wherein nickel ferrite nanoparticles are in the core, covered with the SiO_2. When incorporating Ag nanoparticles over these structures, the size of the aggregates is around 50 micrometers.

4. Conclusions

Sol-gel process provides a successful synthesis of nickel ferrite superparamagnetic nanoparticles coated and functionalized with antimicrobial agents, such as the silver nanoparticles. The characterization of samples at different temperature indicates that heat treatment at 1100°C is needed to obtain high structural crystallinity of the nickel ferrite and this crystallinity has a positive impact on the magnetic properties. The nickel phase obtained by this process was $Ni_{1.43}Fe_{1.7}O_4$.

Among that we obtain aggregates; these are formed with magnetic nanoparticles acting as support agents to fix the Ag nanoparticles over the shell. This configuration allows the composites to be recovered.

Finally, we can conclude that, in order to incorporate silver to the ferrite, our method is simple and results show a successful incorporation; in this sense the possibility to study

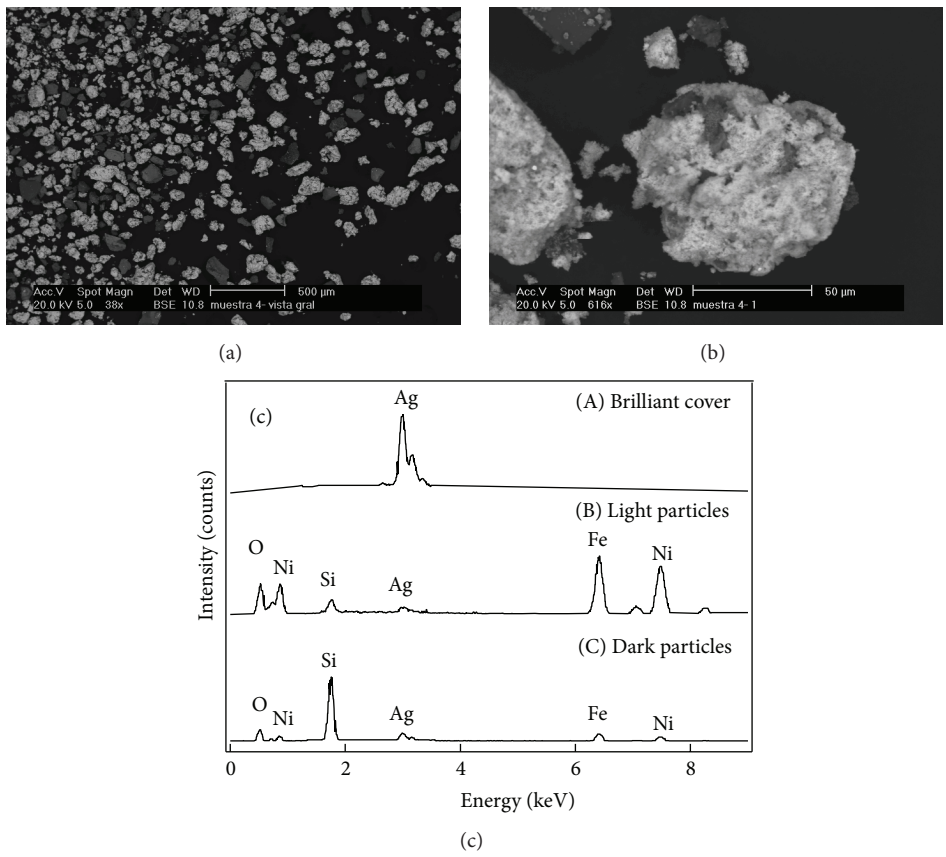

Figure 6: SEM micrographs of nickel ferrite-SiO_2/Ag (a) and (b) and EDS of isolated aggregates (c).

this composite as a disinfectant is clear, with the advantage that it is easily recoverable.

Conflict of Interests

The authors declare that there is no conflict of interests regarding the publication of this paper.

References

[1] F. Sonvico, C. Dubernet, P. Colombo, and P. Couvreur, "Metallic colloid nanotechnology, applications in diagnosis and therapeutics," *Current Pharmaceutical Design*, vol. 11, no. 16, pp. 2091–2105, 2005.

[2] A. Hajdú, E. Tombácz, E. Illés, D. Bica, and L. Vékás, "Magnetite nanoparticles stabilized under physiological conditions for biomedical application," in *Colloids for Nano- and Biotechnology*, vol. 135 of *Progress in Colloid and Polymer Science*, pp. 29–37, Springer, Berlin, Germany, 2008.

[3] L. Chauhan, A. K. Shukla, and K. Sreenivas, "Dielectric and magnetic properties of Nickel ferrite ceramics using crystalline powders derived from DL alanine fuel in sol–gel auto-combustion," *Ceramics International*, vol. 41, no. 7, pp. 8341–8351, 2015.

[4] L. Li, G. Li, R. L. Smith Jr., and H. Inomata, "Microstructural evolution and magnetic properties of $NiFe_2O_4$ nanocrystals dispersed in amorphous silica," *Chemistry of Materials*, vol. 12, no. 12, pp. 3705–3714, 2000.

[5] S.-Y. Yu, H.-J. Zhang, J.-B. Yu, C. Wang, L.-N. Sun, and W.-D. Shi, "Bifunctional magnetic-optical nanocomposites: grafting lanthanide complex onto core–shell magnetic silica nanoarchitecture," *Langmuir*, vol. 23, no. 14, pp. 7836–7840, 2007.

[6] M. C. Blesa, U. Amador, E. Morán, N. Menéndez, J. D. Tornero, and J. Rodríguez-Carvajal, "Synthesis and characterization of nickel and magnesium ferrites obtained from α-$NaFeO_2$," *Solid State Ionics*, vol. 63–65, pp. 429–436, 1993.

[7] M. C. Blesa, E. Morán, N. Menéndez, J. D. Tornero, and C. Torrón, "Hydrolysis of sodium orthoferrite [α-$NaFeO_2$]," *Materials Research Bulletin*, vol. 28, no. 8, pp. 837–847, 1993.

[8] L. Zhang, B. Liu, and S. Dong, "Bifunctional nanostructure of magnetic core luminescent shell and its application as solid-state electrochemiluminescence sensor material," *The Journal of Physical Chemistry B*, vol. 111, no. 35, pp. 10448–10452, 2007.

[9] S. Santra, R. P. Bagwe, D. Dutta et al., "Synthesis and characterization of fluorescent, radio-opaque, and paramagnetic silica nanoparticles for multimodal bioimaging applications," *Advanced Materials*, vol. 17, no. 18, pp. 2165–2169, 2005.

[10] H.-H. Yang, S.-Q. Zhang, X.-L. Chen, Z.-X. Zhuang, J.-G. Xu, and X.-R. Wang, "Magnetite-containing spherical silica nanoparticles for biocatalysis and bioseparations," *Analytical Chemistry*, vol. 76, no. 5, pp. 1316–1321, 2004.

[11] P. Gong, H. Li, X. He et al., "Preparation and antibacterial activity of Fe_3O_4@Ag nanoparticles," *Nanotechnology*, vol. 18, no. 28, Article ID 285604, 2007.

[12] Y. H. Kim, D. K. Lee, H. G. Cha, C. W. Kim, and Y. S. Kang, "Synthesis and characterization of antibacterial Ag-SiO_2

nanocomposite," *Journal of Physical Chemistry C*, vol. 111, no. 9, pp. 3629–3635, 2007.

[13] S. Senapati, S. K. Srivastava, S. B. Singh, and A. R. Kulkarni, "SERS active Ag encapsulated Fe@SiO_2 nanorods in electromagnetic wave absorption and crystal violet detection," *Environmental Research*, vol. 135, pp. 95–104, 2014.

[14] J. Shen, Y. Zhu, X. Yang, J. Zong, and C. Li, "Multifunctional Fe_3O_4@Ag/SiO_2/Au core-shell microspheres as a novel SERS-activity label via long-range plasmon coupling," *Langmuir*, vol. 29, no. 2, pp. 690–695, 2013.

[15] J. Su, Y. Zhang, S. Xu et al., "Highly efficient and recyclable triple-shelled Ag@Fe_3O_4@SiO_2@TiO_2 photocatalysts for degradation of organic pollutants and reduction of hexavalent chromium ions," *Nanoscale*, vol. 6, no. 10, pp. 5181–5192, 2014.

[16] X. Wang, Y. Dai, J.-L. Zou et al., "Characteristics and antibacterial activity of Ag-embedded Fe_3O_4@SiO_2 magnetic composite as a reusable water disinfectant," *RSC Advances*, vol. 3, no. 29, pp. 11751–11758, 2013.

[17] A. S. Savel'eva and O. V. Vodyankina, "Formation of the active surface of Ag/SiO_2 catalysts in the presence of FeO_x additives," *Russian Journal of Physical Chemistry A*, vol. 88, no. 12, pp. 2203–2208, 2014.

[18] R. Soleyman, A. Pourjavadi, N. Masoud, and A. Varamesh, "Core-shell γ-Fe_2O_3/SiO_2/PCA/Ag-NPs hybrid nanomaterials as a new candidate for future cancer therapy," *International Journal of Nanoscience*, vol. 13, no. 1, Article ID 1450008, 2014.

[19] C.-L. Fang, K. Qian, J. Zhu, S. Wang, X. Lv, and S.-H. Yu, "Monodisperse α-Fe_2O_3@SiO_2@Au core/shell nanocomposite spheres: synthesis, characterization and properties," *Nanotechnology*, vol. 19, no. 12, Article ID 125601, 2008.

[20] I. G. Blanco-Esqueda, G. Ortega-Zarzosa, J. R. Martínez, A. L. Guerrero-Serrano, and J. A. Matutes-Aquino, "Formation and characterization of γ-Fe_2O_3@SiO_2@Ag," *Journal of Sol-Gel Science and Technology*, vol. 74, no. 3, pp. 734–739, 2015.

[21] J. R. Martínez, F. Ruiz, Y. V. Vorobiev, F. Pérez-Robles, and J. González-Hernández, "Infrared spectroscopy analysis of the local atomic structure in silica prepared by sol-gel," *Journal of Chemical Physics*, vol. 109, no. 17, pp. 7511–7514, 1998.

[22] M. Ferrari and L. Lutterotti, "Method for the simultaneous determination of anisotropic residual stresses and texture by X-ray diffraction," *Journal of Applied Physics*, vol. 76, no. 11, pp. 7246–7255, 1994.

[23] S. A. Palomares Sánchez, S. Ponce-Castañeda, J. R. Martínez, F. Ruiz, Y. Chumakov, and O. Domínguez, "Quantitative analysis of iron oxide particles embedded in an amorphous xerogel matrix," *Journal of Non-Crystalline Solids*, vol. 325, no. 1–3, pp. 251–257, 2003.

[24] C. C. Tsai, J. R. Nemanich, and M. J. Thompson, "Interfacial reactions between Au and hydrogenated amorphous Si," *Journal of Vacuum Science & Technology*, vol. 21, p. 632, 1982.

[25] M. Seibt, S. Buschbaum, U. Gnauert, W. Schröter, and D. Oelgeschläger, "Nanoscale observation of a grain boundary related growth mode in thin film reactions," *Physical Review Letters*, vol. 80, no. 4, pp. 774–777, 1998.

[26] A. Le Bail, "Modelling the silica glass structure by the Rietveld method," *Journal of Non-Crystalline Solids*, vol. 183, no. 1-2, pp. 39–42, 1995.

[27] B. H. Toby, "R factors in Rietveld analysis: how good is good enough?" *Powder Diffraction*, vol. 21, no. 1, pp. 67–70, 2006.

[28] J. R. Martínez and F. Ruiz, "Mapeo estructural de sílica xerogel utilizando espectroscopía infrarroja," *Revista Mexicana de Física*, vol. 48, no. 2, pp. 142–149, 2002.

[29] K. Kandori, N. Ohkoshi, A. Yasukawa, and T. Ishikawa, "Morphology control and texture of hematite particles by dimethylformamide in forced hydrolysis reaction," *Journal of Materials Research*, vol. 13, no. 6, pp. 1698–1706, 1998.

[30] S. Ponce-Castañeda, J. R. Martínez, F. Ruiz, S. Palomares-Sánchez, and O. Domínguez, "Synthesis of Fe_2O_3 species embedded in a silica xerogel matrix: a comparative study," *Journal of Sol-Gel Science and Technology*, vol. 25, no. 1, pp. 29–36, 2002.

[31] A. Duran, C. Serna, V. Fornes, and J. M. Fernández-Navarro, "Sol-gel transition in simple silicates II," *Journal of Non-Crystalline Solids*, vol. 63, pp. 45–59, 1984.

[32] J. F. Pérez-Robles, F. J. García-Rodríguez, J. González-Hernández et al., "Optical characterization of Fe- and Cu-doped SiO_2 glasses prepared by the sol-gel method," in *Optical Diagnostics of Materials and Devices for Opto-, Micro-, and Quantum Electronics 1997, 947200*, vol. 3359 of *Proceedings of SPIE*, April 1998.

[33] N. B. Colthup, L. H. Daly, and S. E. Wiberly, *Introduction to Infrared and Raman Spectroscopy*, Academic Press, New York, NY, USA, 2nd edition, 1975.

[34] G. Orcel, J. Phalippou, and L. L. Hench, "Structural changes of silica xerogels during low temperature dehydration," *Journal of Non-Crystalline Solids*, vol. 88, no. 1, pp. 114–130, 1986.

[35] G. Ortega-Zarzosa, J. R. Martínez, A. Robledo-Cabrera, G. A. Martínez-Castañón, M. G. Sánchez-Loredo, and F. Ruiz, "Annealing behavior of silica gel powders modified with silver crystalline aggregates," *Journal of Sol-Gel Science and Technology*, vol. 27, no. 3, pp. 255–262, 2003.

[36] M. Mandal, S. Kundu, S. K. Ghosh et al., "Magnetite nanoparticles with tunable gold or silver shell," *Journal of Colloid and Interface Science*, vol. 286, no. 1, pp. 187–194, 2005.

[37] J. Garcia-Torres, E. Vallés, and E. Gómez, "Synthesis and characterization of Co@Ag core—shell nanoparticles," *Journal of Nanoparticle Research*, vol. 12, no. 6, pp. 2189–2199, 2010.